Spatially Explicit Coupled Map Lattice Simulation of Malaria Transmission in the Brazilian Amazon

Anthony E. Kiszewski[1], Marcia Castro[2] and Sarah McGough[2]
[1]*Natural and Applied Sciences, Bentley University, 175 Forest Street, Waltham, MA, U.S.A.*
[2]*Harvard T.H. Chan School of Public Health, 677 Huntington Avenue, Boston, MA, U.S.A.*

Keywords: Malaria, Mosquito, Cellular Automata, Coupled Map Lattice, Spatially Explicit, Individual-based.

Abstract: End stage malaria elimination efforts will require interventions against transmission that is sparse, cryptic and spotty, situations suited for explicitly spatial simulation. A simulation of mosquito population dynamics and *Plasmodium vivax* malaria transmission in the Brazilian Amazon is described combining techniques of cellular automata and coupled map lattices. Within a 200x200 grid, 64 dispersed communities of 50 households each are represented with larval breeding sites following a random Gaussian distribution. Discrete representation of individual humans allows examination of the effect of circulation and migration. Continuous representation of mosquito abundance allows for more realistic scaling over space. Simulations (n=100) reach equilibrium within 200 daily time steps. Adult mosquito populations range between 230-241,000 individuals. An average parous rate of 56.5% for stable mosquito populations is consistent with values reported in local field studies of the primary vector, *Anopheles darlingi*. Equilibrium prevalence of *P. vivax* infections averages 3% (1.8-3.9%) and is highly sensitive to treatment seeking behaviour of asymptomatics. This simulation provides a stable platform that may be useful for investigating the role of human migration and asymptomatic malaria in perpetuating transmission cycles in this region and interventions supporting malaria elimination efforts.

1 INTRODUCTION

Plasmodium vivax is currently the dominant species of malaria in the Brazilian Amazon (Barbosa et al. 2014). While less dangerous than *P. falciparum,* infections cause recurrent attacks that impose enormous impacts on the health and economic potential of residents (Mendis et al. 2001).

Certain areas of the Amazon have reported promising declines of both *P. falciparum* and *P. vivax* transmission (Barbosa et al. 2014, Vitor-Silva et al. 2016), However, asymptomatic infections challenge malaria elimination efforts because there is less incentive to seek treatment in the absence of symptoms. Asymptomatic infections can persist and remain infectious for many months in the absence of treatment (Tripura et al. 2016).

Anopheles darlingi is the dominant vector of malaria in the Brazilian Amazon (Castro et al. 2006, Pimenta et al. 2015). Anthropogenic changes to the natural landscape have only increased its role in maintaining malaria transmission cycles (Vittor et al. 2006, 2009) in settlement areas.

Local migration into, from and between (i.e. circulation) Amazonian communities may serve to disperse and perpetuate foci of transmission (Martens and Hall 2000). Residents of Amazonia are highly mobile, colonizing new areas and circulating on a daily, seasonal and periodic basis within settled communities in pursuit of labor and trade (Camargo et al. 1994; McGreevy et al. 1989).

Such movements have the potential to perpetuate malaria transmission by repopulating extinct foci with new parasites from transmission 'hot spots.' Thus, these activities also pose a challenge to malaria elimination efforts.

Individual-based models allow the study of patchiness and non-random dispersal on the dynamics of disease transmission (Auger et al. 2008, de Castro et al. 2011), important factors where transmission is low and locality-dependent. Thus, we developed an explicitly spatial simulation that captures key features of malaria transmission in this region including the behavior of *An. darlingi*, human population distribution and mobility, intraspecific competition

Kiszewski, A., Castro, M. and McGough, S.
Spatially Explicit Coupled Map Lattice Simulation of Malaria Transmission in the Brazilian Amazon.
DOI: 10.5220/0006862701120119
In *Proceedings of 8th International Conference on Simulation and Modeling Methodologies, Technologies and Applications (SIMULTECH 2018)*, pages 112-119
ISBN: 978-989-758-323-0

among larvae and the frequency of asymptomatic carriage of infectious parasites.

We aimed to create a platform in which to explore surveillance and intervention strategies to achieve local elimination of malaria in South America, and to assess the advantages of a hybrid automata/couple map lattice approach.

2 METHODS

This simulation was encoded using the J functional programming language (Jsoftware v. 8.06), a platform optimized for matrix manipulations. Simulations were executed on an ASUS Zenbook laptop (16 GB RAM) running Windows 10.

We combined techniques used in cellular automata and "coupled map lattices," an "n"-dimensional lattice where each site evolves in time through a map (or recurrence equation) of the form:

$$\mathbf{X}^{t+1} = F(\mathbf{X}^t) \quad (1)$$

X represents all values in the n-dimensional lattice at time (t) and F(**X**) represents the set of functions describing its transition over time. Time (t) advances in discrete units of 12 hours. Each "k" (overlay) dimension of the matrix **X** contains information about the i,j (row, column) locations of each variable, including larval mosquito stage, adult feeding and gonotrophic state, and breeding site characteristics. Dispersal of adult mosquitoes beyond their i,j locations occurs over an 8 cell Von Neumann neighbourhood.

Multiple superimposed and interacting matrices were used to track variables representing larval mosquito habitats, human households, and mosquitoes and humans in various stages of malaria infection. A hybrid numerical approach was employed in which humans and disease states were tracked as discrete integers while mosquito population dynamics and dispersal were represented by continuous values representing the number of mosquitoes per location.

The simulation environment was modeled after the perennial malaria transmission occurring in and around Remansinho, a settlement project in southern Amazonas State near the borders of Acre and Rondonia. Each cell on the matrix represents an area of about 100 m^2 for a total simulated area of 4 km^2.

Bodies of water representing suitable larval habitats are randomly and Gaussian distributed across a 200x200 cell matrix. All are assumed to be of equal depth and surface area and begin with equal nutrient resources and cycling. For the purposes of the present simulation such bodies are assumed to be permanent.

The primary mosquito vector, *An. darlingi,* is adapted to breeding on the margins of rivers, particularly in seasons when rivers flood. It has also been associated with anthropogenic environmental changes, breeding behind impoundments caused by road construction through wetland environments (Rufalco-Moutinho et al. 2016).

Climatic variability is not explicitly depicted. Thus, temperatures are held constant using the average temperature at the end of rainy season in Remansinho (26^{o}C www.worldclim.org).

2.1 Human Population

Aerial photos provided a template for the simulation's depiction of settlement density. Patterns derived were used to create a basic unit representing a community of 50 households along a roadway. These tiles were tessellated evenly across the matrix, creating a total of 64 identical 'communities' for a total of 3,200 households. Initial household sizes and births correspond to survey data collected near Remansinho but constrained to a maximum of eight permanent residents per household. The maximum population supported by this layout is thus 25,600 people.

Migration and circulation is simulated by shifting people between communities. Out-migration and returns occur on a stochastic basis with outcomes determined by lottery draw from a uniform distribution. People who leave a particular household always return to the same household, although the duration of their absence can vary. Up to two household members can be absent at any given time. Visitors to households are not constrained by the eight member per household limitation.

2.2 Mosquito Population

2.2.1 Adults

Anopheles darlingi is the sole mosquito vector species considered in these simulations. Separate matrices of continuous variables track adult mosquitoes by stage of gonotrophic cycle (host-seeking, bloodfed, gravid, ovipositing) and day of extrinsic incubation, if infected.

Dispersal is weighted towards households when mosquitoes are in a host-seeking state and towards larval habitats when they are gravid. Dispersal in the absence of environmental cues occurs evenly to all adjoining sites on the matrix. Bloodfed, resting mosquitoes do not disperse (Hiwat and Bretas 2011).

2.2.2 Subadult Mosquitoes

Larvae only occur on sites where suitable habitats are present, as indicated by a reference matrix depicting the locations of such habitats (Figure 1). Oviparous mosquitoes deposit ova only in such sites.

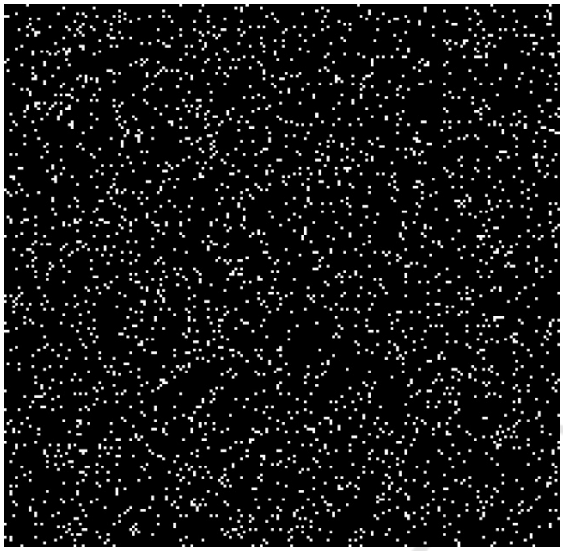

Figure 1: Distribution of larval mosquito habitats. Bodies of water (white) supporting mosquito larvae are distributed randomly via a Gaussian algorithm to 20% of grid sites.

Separate state matrices track larval stages or 'instars' by stage of development. Daily mortality rates derived from life table data (Araujo et al. 2012) are specific to instar. Larval population dynamics are constrained by density-dependent intraspecific interactions (Klomp 1964). Carrying capacity is dynamic and emergent, deriving from nutrient limitations in larval habitats.

When nutrients are not limiting, larvae advance in the optimal period expected at 26ºC for *An. darlingi,* approximately 12 days on average (Bergo et al. 1990). When nutrients are lacking, larval development is delayed until nutrients become available (Bar-Zeev 1957, Araújo et al. 2012).

Nutritional content of larval habitats is assumed to fluctuate in response to utilization by larvae, inflow from external sources as well as internal inputs resulting from microbial decomposition or algal photosynthesis. Each day, there is also a negative nutrient flux independent of mosquito larval activity related to uptake by other organisms, sedimentation, decay or other factors.

Mosquito larvae compete for nutrients with a precedence favoring older instars. Heuristically, but based on larval studies (Dahl et al. 1993), 30% of the available nutriment is assumed to consumed non-competitively at the rate of 2, 4, 8 and 16% for first through fourth larval instars respectively. The remaining nutritive content of the site is then obtained competitively with priority given to older instars.

2.3 Malaria Transmission

2.3.1 Mosquito to Human

Daily transmission of malaria from mosquitoes to humans is a function of the number of infected mosquitoes a person is likely to contact within a twenty-four hour period. Specifically, the probability of a person acquiring a malaria infection each day is governed by the expression:

$$P_{inf(h)} = 1 - (1-i_m)^{nba} \quad (2)$$

where: i_m = probability that a single infectious mosquito bite triggers a patent malaria infection in a person.
n = number of infectious mosquitoes per person in a given household.
b = biting success (daily probability that an infectious mosquito is successful in obtaining a blood meal from hosts in its vicinity).
a = anthropophagy (the probability that an infectious mosquito obtains a blood meal from a person and not an animal).

Humans are handled as discrete and individual entities in this simulation with integers representing infection states. $P_{inf(h)}$ is used to determine the probability of a state transition from uninfected to infected. This transition is thus executed for only those individuals for which a random number from a uniform distribution between 0 and 1 is less than or equal to the probability of infection. Thereafter, infections states for each household member change on a daily basis to represent advancing prepatency.

Risk of acquiring malaria infections is assumed to be independent of age, as is typical in areas with seasonal malaria transmission and moderate prevalence rates (Hay et al. 2004).

2.3.2 Human to Mosquito

The proportion of mosquitoes in a given site acquiring a malaria infection each day is governed by the expression:

$$P_{inf(m)} = i_h pba \quad (3)$$

where: i_h = probability that a mosquito feeding on an infectious human becomes infected.

p = proportion of humans in a site infectious with malaria.

b = biting success (daily probability that a mosquito is successful in obtaining a blood meal).

a = anthropophagy (the probability that an infectious mosquito obtains a blood meal from a person and not an animal).

We assume that all humans bearing patent malaria infections are equally infectious to mosquitoes and that asymptomatic infections remain asymptomatic.

Using Moshkovsky's formula for extrinsic incubation of *P. vivax* malaria parasites (Detinova 1962), we assume that infected mosquitoes exposed to an average ambient outdoor temperature of 26°C would require about 9.13 days (E = 105/T-14.5) to become infectious.

2.3.3 Intrinsic Incubation

Humans are assigned a discrete integer state corresponding to their malaria infection status, with 1 representing uninfected individuals, 2-15 representing each day of prepatency for infected individuals, 16 representing those presenting with clinical symptoms and 17 representing asymptomatic individuals. All patent infections are assumed to be infectious to vectors.

Loss of infection can occur with or without treatment with infected individuals returning to their initial state. For this hypoendemic situation, we do not assume the presence of sufficient immunity to alter the probability of re-infection. The current simulation also does not account for superinfection by parasites in differing developmental stages.

2.4 Sensitivity Analyses

Model parameters, whenever possible, were extracted from literature appropriate to the area targeted in the simulation or drawn directly from survey data (Table 1). Simulations using random sets of all input variables were used to explore the parameter space and determine the range of outcomes possible, including human, mosquito and parasite population dynamics and infection rates. Scatter plots were generated to track the effect of diverse sets of randomly sampled model input distributions on each output variable.

Table 1: Baseline Parameter Assumptions and Sources.

Parameter		Value	Range	Source
Mosquito	Immature Survival Rate (daily)			
	1st instar	0.80	0.75-0.85	Araujo et al. 2012
	2nd instar	0.90	0.85-0.95	"
	3rd instar	0.92	0.85-0.95	"
	4th instar	0.95	0.92-0.98	"
	Pupae	0.95	0.92-0.98	"
	Immature Development Period			
	12 days			Gu and Novak 2006
	Mosquito Infection – Extrinsic Incubation			
	P. vivax	10 days	9-11 days	Paaijmans et al. 2009
	Human Blood Index	0.458	0.40-0.50	Kiszewski et al. 2004
Trans-mission				
	Prob. of trans. to human		0.05-0.13	Krafsur and Armstrong 1978
	Prob. of trans. to mosquito		0.1-0.6	Muirhead-Thomson 1954, 1957; Rutledge et al. 1969
	Intrinsic Incub. Period		9-12 days	Molineaux and Gramiccia 1980
	Infectious period (no treatment)	18 mos.	12-24 months	Bloland and Williams 2002

Elimination did not occur within the range of natural conditions without external forcing or intervention. Elimination of parasite populations occurred in some runs when treatment rates of asymptomatic carriers were equal or greater than symptomatics. No parameter sets led to outcomes that could not be explained by natural interactions. Adult mosquito survival rate and treatment rate among asymptomatic humans had the strongest effect on equilibrium prevalence of infection in humans and mosquitoes, while variables affecting larval abundance had the least impact.

3 RESULTS

Parameters selected within reported ranges of natural values (Table 1) delivered plausible outcomes.

Multiple runs (n=100) showed variable but stable results between simulations without extreme variation (Table 2).

Table 2: Mean equilibrium values for primary outcome variables using default parameters. (n = 100, 1,000 time steps).

Variable	Mean/ 95% CI.	SD	Min	Max
Human population	9,416.8 (9402.2, 9431.4)	73.4	9,259	9,593
No. People infected	279.35 (271.02, 287.68)	41.98	170	365
% Prevalence	2.97 (2.88, 3.06)	0.45	1.82	3.89
Asympt. Infections	236.66 (229.68, 243.64)	35.19	143	313
% Asympt.	93.06 (92.76, 93.37)	1.55	89	96
Subadult Mosquitoes (x 10^7)	1.64 (1.64-1.65)	0.03	1.58	1.71
Adult Mosquitoes	230,451 (229,595, 231,306)	4,310	220,524	241,256
Infected Mosquitoes	1,394.7 (1,348.6, 1,440.8)	232.2	789	2018.3
Sporozoite Rate	0.61 (0.59, 0.62)	0.1	0.34	0.88
% Parous	56.51 (56.42, 56.61)	0.48	55.46	57.82

The total population of humans in this simulation reaches about 9,417 on average, with a minimum of 9,259 and a maximum of 9,593. Adult mosquitoes reach a mean population size of 230,451 (with a range of 220,524 to 241,256). These values correspond to a mosquito/human ratio of about 24:1.

Most outcome variables reach equilibrium in about 400 time steps. Point prevalence of malaria infection settles at about 3% on average. Other measures of transmission stability independent of infection, such as parous rate, reach equilibrium more quickly, achieving stable oscillations in about 200 time steps.

Baseline parameters produced lower prevalence (3%) than reported for *P. vivax* for Amazonia as a whole (5.3%) and Rondonia in particular (4.9%, Arruda et al. 2007), and significantly less than that reported at Remansinho (9.1%, Barbosa et al. 2014).

An alternative set of parameters employing a slightly different treatment rate in asymptomatic humans (0.25% treatment probability per day vs. 0.5%) brought equilibrium prevalence into these observed ranges (6.2%) while keeping vector sporozoite rates below 1%.

The number of infected mosquitoes at equilibrium (Table 2) averages about 1,394 (789-2,018). As one might expect, there was a strong correlation between infected mosquitoes and infected humans ($R = 0.904$, $P<0.001$). Abundance of subadult mosquitoes was not significantly correlated with human malaria infections ($R = 0.19$, $P=0.059$) unlike adult mosquito abundance ($R = 0.26$, $P=0.008$).

Mosquito parous rates do not reach equilibrium, but rather oscillate stably around a mean of about 54.6% even in runs in excess of one thousand time steps. This value for parity is slightly higher than the range observed in natural, stable populations of *An. darlingi* (Moreno et al. 2007; Rubio-Palis et al. 2013). Parity in wild mosquito populations tend to be observed below 50% except during seasons when populations are growing after a seasonal interruption.

4 CONCLUSIONS

The baseline parameters of this simulation deliver outcomes for both human and mosquito malaria infection dynamics comparable to those observed within the study areas we are attempting to simulate.

The age structure of mosquito vector populations as indicated by parous rate is a critical determinant of vectorial capacity and a sensitive indicator of the efficacy of anti-vector interventions. Our baseline value of 56.5% is slightly elevated over empirical observations of *An. darlingi* in the region (Moreno et al. 2007, de Barros et al. 2011). Baseline sporozoite rates of less than 1% are also consistent with local observations (Hiwat and Bretas 2011).

While the simulated prevalence rate for *P. vivax* malaria infection was significantly less than what was recently reported from the targeted study area at Remasinho in southern Amazonas, prevalence values can differ widely between localities and seasons. Significant shifts in prevalence have been observed even in the same areas over the course of a few years (Barbosa et al. 2014). Modest changes in treatment rate among asymptomatic people led to simulated

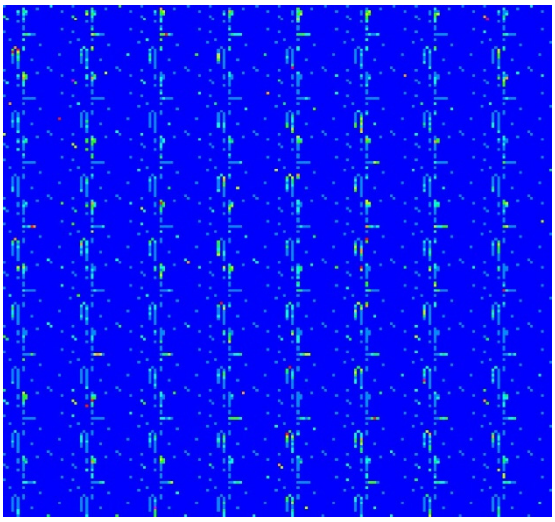

Figure 2: Distribution of households and malaria cases. Light blue represents households without malaria. Other colors (green to red) indicate the presence of malaria in at least one household member.

prevalence rates within the ranges reported in surveys.

Malaria surveys in Amazonia suggest that asymptomatic malaria infections far outnumber symptomatic infections. While the ratio of symptomatic to asymptomatic infections produced by this simulation conforms to these observations, the ratio we produced (5.54 asymptomatic for every symptomatic person) is close to the 4-5X range observed in some empirical studies (Alves et al. 2002).

Prevalence of parasites in humans and vectors was highly sensitive to the presence of asymptomatic infections. Such cases may be a critical target for elimination campaigns because their presence helps perpetuate transmission and asymptomatic individuals may be less likely to self-report infections and seek treatment than those experiencing acute symptoms of malaria. Active surveillance will be required to identify these cases.

Other individual or agent-based models have been successful at reproducing the spatial dynamics of malaria transmission (Bomblies et al. 2008, Gu and Novak 2009, Zhou et al. 2010, Eckhoff 2011, Zhu et al. 2015, Pizzitutti et al. 2015) including some aspects of human mobility (Zhu et al. 2015, Pizzitutti et al. 2018). The model presented here is distinct from most prior efforts in its detailed simulation of larval population dynamics. With few exceptions (Bomblies et al. 2009), most simulations impose carrying capacity by increasing mortality or limiting oviposition in crowded habitats. The present model allows carrying capacity and larval development rate to fluctuate in response to crowding. Thus, it captures the paradoxical effect of enhanced pupal productivity after 'thinning' by insecticidal interventions (Agudelo-Silva and Spielman et al. 1984), and is thus well suited for evaluating the impacts of anti-larval interventions. The mechanism for regulating mosquito population growth in this simulation was based on the concept of niche partitioning (Gilbert et al. 2008) via intraspecific nutrient selectivity by larval instars (Klomp 1964, Merritt 1987, Dahl et al. 1993).

The current model also allows depiction of circulation of people to other communities with overnight stays of variable length with return to their original households. Prior efforts (Pizzitutti et al. 2018) simulate diurnal activities with daily return to households of origin. Thus, the influence of temporary migration in creating new hot-spots and perpetuating malaria transmission in the face of elimination campaigns can be assessed. The present model also depicts differences in treatment-seeking behavior in symptomatic and asymptomatic humans which can further facilitate perpetuation of malaria.

One drawback of our modeling approach as currently formulated is its inflexibility with regards to simulating climatic variability. Scenarios exploring climatic changes are possible with this technique, but require alternative versions to the code for a particular set of climatic conditions. Because time is discrete and variables representing infection status represent specific days of incubation, any changes in extrinsic incubation period requires changes in the code to provide additional or fewer classes of incubation states. As such, the current model is best applied to shorter time scales where climatic conditions remain stable.

Other refinements of this model might include allowing vectors multiple chances to feed over the course of a single gonotrophic cycle. Such feeding behavior has been observed with *An. darlingi* in natural situations (de Oliveira et al. 2012). The authors of this work even observed some mosquitoes feeding more than once in the course of a single day.

Thus, the present study suggests that our simulation approach provides a stable and relatively realistic platform for evaluations of malaria interventions. We hope in particular to exploit the features of the current model to explore strategies designed to eliminate transmission in hypo- and mesoendemic areas, including practices not generally undertaken or recommended where transmission is hyperendemic.

Upon incorporating the refinements suggested by these preliminary evaluations, the simulation will be applied to several contrasting intervention scenarios. These will include larval source reductions as part of a broader strategy of integrated vector management and mass drug administration in communities. We also hope to explore in detail the role of human migration and asymptomatic malaria in perpetuating transmission cycles in this region towards maximizing the impact of malaria elimination efforts.

ACKNOWLEDGEMENTS

We thank Dr. Susana Barbosa of the Department of Parasitology, Institute of Biomedical Sciences, University of São Paulo, São Paulo, Brazil for her helpful consultations in developing this model.

REFERENCES

Agudelo-Silva F, Spielman A. 1984. Paradoxical effects of simulated larviciding on production of adult mosquitoes. Am J Trop Med Hyg. 33:1267-1269.

Alves FP, Durlacher RR, Menezes MJ, Krieger H, Pereira da Silva L. 2002. High prevalence of asymptomatic *Plasmodium vivax* and *Plasmodium falciparum* infections in native Amazonian populations. Am J Trop Med Hyg. 66:641–648.

Araujo M, Gil L, Silva A. 2012. Larval food quality affects development time, survival and adult biological traits that influence the vectorial capacity of *Anopheles darlingi* under laboratory conditions. Malaria J. 11:261. doi:10.1186/1475-2875-11-261.

Arruda ME, Zimmerman RH, Souza RMC, Oliveira-Ferreira, J. 2007. Prevalence and level of antibodies to the circumsporozoite protein of human malaria parasites in five states of the Amazon region of Brazil. *Memórias do Instituto Oswaldo Cruz*, *102*:367-372.

Auger P, Kouokam E, Sallet G, Tchuente M, Tsanou B. 2008. The Ross-MacDonald model in a patchy environment. *Mathem. Biosci.* 216:1232-12131.

Bar-Zeev M. 1957. The effect of density on the larvae of a mosquito and its influence on fecundity. *Bull Res Council Israel, Sec B*. 6:220-228.

Barbosa S, Gozze AB, Lima NF, Batista CL, da Silva Bastos M, Nicolete VC, Fontoura PS et al. 2014. Epidemiology of disappearing *Plasmodium vivax* malaria: a case study in rural Amazonia. *PLoS NTDs.* 8:e3109.

Bergo, Eduardo Sterlino, Buralli, Geraldo Magela, Santos, Jair Licio Ferreira, & Gurgel, Sergio Mello. (1990). Avaliação do desenvolvimento larval de *Anopheles darlingi* criado em laboratório sob diferentes dietas. *Revista de Saúde Pública*, *24*(2), 95-100.

Bloland PB, Williams HA. 2002. Malaria control during mass population movements and natural disasters: Committee on Population (CPOP). *National Academies Press.* 184 pp.

Bomblies A, Duchemin J-B, Eltahir EAB. 2009. A mechanistic approach for accurate simulation of village scale malaria transmission. Malaria J. 8:223. doi:10.1186/1475-2875-8-223.

Camargo LMA, Ferreira MU, Krieger H, De Camargo EP, Da Silva LP. 1994. Unstable hypoendemic malaria in Rondonia (Western Amazon region, Brazil): epidemic outbreaks and work-associated incidence in an agro-industrial rural settlement. *Am J Trop Med Hyg.* 51:16-25.

Castro MC, Monte-Mór RL, Sawyer DO, Singer, BH. 2006. Malaria risk on the Amazon Frontier. *PNAS.* 103: 2452-2457.

Charlwood JD, Alecrim WA. 1989. Capture-recapture studies with the South American malaria vector *Anopheles darlingi*, Root. *Ann Trop Med Parasitol.* 83:569-576.

Dahl C, Sahlen G, Johannisson A, Amneus H. 1993. Differential particle uptake by larvae of three mosquito species (Diptera:Culicidae). *J. Med Entomol.* 30:537-543.

de Barros FSM, Honorio NA, Arruda ME. 2011. Survivorship of *Anopheles darlingi* (Diptera:Culicidae) in relation with malaria incidence in the Brazilian Amazon. *PLoS One.* 6: e22388.

de Castro Medeiros LC, Castilho CAR, Braga C, de Souza WV, Regis L, Monteiro AMV. 2011. Modeling the dynamic transmission of dengue fever: investigating disease persistence. *PLoS NTDs.* 5:e942.

de Oliveira CD, Tadei WP, Abdalla FC, Paolucci Pimenta PF, Marinotti O. 2012. Multiple blood meals in *Anopheles darlingi* (Diptera:Culicidae). *J Vector Ecol.* 37:351-8. doi:10.1111/j.1948-7134.2012.00238.x.

Detinova, TS. 1962. Age-grouping methods in Diptera of medical importance, with special reference to some vectors of malaria. *Geneva : WHO*.

Eckhoff PA. 2011. A malaria transmission-directed model of mosquito life cycle and ecology. Malaria J. 10:303.

Gilbert B, Srivastava DS, Kirby KR. 2008. Niche partitioning at multiple scales facilitates coexistence among mosquito larvae. *Oikos.* 117:944-50.

Gu W, Novak RJ. 2006. Statistical estimation of degree days of mosquito development under fluctuating temperatures in the field. *J Vec Ecol.* 31:107-112.

Gu W, RJ Novak. 2009. Agent-based modelling of mosquito foraging behaviour for malaria control. Trans R Soc Trop Med Hyg. 103:1105. doi:10.1016/j.trstmh.2009.01.006.

Hay SI, Guerra CA, Tatem AJ, Noor AM, Snow RW. 2004. The global distribution and population at risk of malaria: past, present, and future. *The Lancet, Infectious Diseases*. 4:327-336. doi:10.1016/S1473-3099(04)01043-6.

Hiwat H, Bretas G. 2011. Ecology of Anopheles darling Root with respect to vector importance: a review. Parasit Vectors. 4:177. doi:10.1186/1756-3305-4-177.

Kiszewski AE, Mellinger A, Spielman A, Malaney P, Sachs SE et al. 2004. A global index representing the stability of malaria transmission. *Am J Trop Med Hyg*. 70: 486-498.

Klomp H. 1964. Intraspecific competition and the regulation of insect numbers. *Ann. Rev. Entomol.* 9:17-40.

Krafsur ES, Armstrong J. 1978. An integrated view of entomological and parasitological observations on falciparum malaria in Gambela, western Ethiopian lowlands. *Trans R Soc Trop Med Hyg.* 72: 348-356.

Martens P, Hall L. 2000. Malaria on the Move: Human Population Movement and Malaria Transmission. *Emerg Inf Dis*. 6:103-109.

McGreevy PB, Dietze R, Prata A, Hembree SC. 1989. Effects of immigration on the prevalence of malaria in rural areas of the Amazon basin of Brazil. *Memorias do Instituto Oswaldo Cruz.* 84:485-91.

Mendis K, Sina BJ, Marchesini P, Carter R. 2001. The neglected burden of *Plasmodium vivax* malaria. *Am J Trop Med Hyg.* 64S:97–106.

Merritt RW. 1987. Do different instars of *Aedes triseriatus* feed on particles of the same size? *JAMCA.* 3:94-96.

Molineaux L, Grammiccia G. 1980. The Garki Project: research on the epidemiology and control of malaria in the Sudan savanna of West Africa. *Geneva: WHO.* 311pp.

Moreno JE, Rubio-Palis Y, Paez E, Perez E. 2007. Abundance, biting behavior and parous rate of anopheline mosquito species in relation to malaria incidence in gold-mining areas of southern Venezuela. *Med Vet Entomol.* 21:339-349.

Muirhead-Thomson RC. 1954. Factors determining the true reservoir of infection of *Plasmodium falciparum* and *Wuchereria bancrofti* in a West African village. *Trans R Soc Trop Med Hyg.* 48:208-225.

Muirhead-Thomson RC. 1957. The malarial infectivity of an African village population to mosquitoes (*Anopheles gambiae*). *Am J Trop Med Hyg.* 6:971-979.

Paaijmans KP, Read AF, Thomas MB. 2009. Understanding the link between malaria risk and climate. *PNAS.* 106:13844-13849.

Pimenta PFP, Orfano AS, Bahia AC, Duarte APM, Rios-Velasquez CM, Melo FF, Pessoa FAC et al. 2015. An overview of malaria transmission from the perspective of Amazon *Anopheles* vectors. Mem Inst Oswaldo Cruz, Rio de Janeiro. 110:23-47.

Pizzitutti F, Pan W, Feingold B, Zaitchik B, Alvarez CA, Mena CF. 2018. Out of the net: an agent-based model to study human movements influence on local-scale malaria transmission. PLoS One. 13(3):e0193493. Doi:10.1371/journal.pone.0193493.

Pizzitutti F, Pan W, Barbieri A, Miranda J, Feingold B, Guedes GR, Alarcon-Valenzuela J, Mena CF. 2015. A validated agent-based model to study the spatial and temporal heterogeneities of malaria incidence in the rainforest environment. Malaria J. 14:514/ doi:10.1186/s12936-015-1030-7.

Rubio-Palis Y, Bevilaqua M, Medina D, Martinez A. 2013. Malaria entomological risk factors in relation to land cover in the Lower Caura River Basin, Venezuela. *Memorias do Instituto Oswaldo Cruz.* 108:220-8.

Rufalco-Moutinho P, Schweigmann N, Pimentel Bergamaschi D, Mureb Sallum MA. 2016. Larval habitats of *Anopheles* species in a rural settlement on the malaria frontier of southwest Amazon, Brazil. *Acta Tropica.* 164:243-258.

Rutledge LC, Gould DJ, Tantichareon B. 1969. Factors affecting the infection of anophelines with human malaria in Thailand. *Trans R Soc Trop Med Hyg.* 63:613-661.

Tripura R, Peto TJ, Chalk J, Lee SJ, Sirithiranont P, Nguon C, Dhorda M, von Seidlein L, Maude RJ et al. 2016. Persistent *Plasmodium falciparum* and *Plasmodium vivax* infections in a western Cambodian population: implications for prevention, treatment and elimination strategies. *Malaria J.* 15:181.

Vitor-Silva S, Siqueira AM, de Souza Sampaio V, Guinovart C, Reyes-Lecca RC, de Melo GC et al. 2016. Declining malaria transmission in rural Amazon: changing epidemiology and challenged to achieve elimination. *Malaria J.* 15:26.

Vittor AY, Gilman RH, Tielsch J, Glass G, Shields T, et al. 2006. The effect of deforestation on the human biting rate of *Anopheles darlingi*, the primary malaria vector of falciparum malaria in the Peruvian Amazon. Am J Trop Med Hyg. 74:3-11.

Vittor AY, Pan W, Gilman RH, Tielsch J, Glass G, et al. 2009. Linking deforestation to malaria in the Amazon: characterization of the breeding habitat of the principal malaria vector, *Anopheles darlingi*. Am J Trop Med Hyg. 81:5-12.

Zhou Y, Arifin SMN, Gentile J, Kurtz SJ, Davis GJ, Wendelberger BA. 2010. An agent-based model of the *Anopheles gambiae* mosquito lifecycle. In summer simulation mutliconference, Ottawa, Ontario, Canada: Society for Computer Simulation International. p. 201-208.

Zhu L, Qualls WA, Marshall JM, Arheart KL, McManus JW et al. 2015. A spatial individual-based model predicting a great impact of copious sugar sources and resting sites on survival of *Anopheles gambiae* and malaria parasite transmission. Malaria J. 14:59.